

SCIENTIFIC REPORTS

OPEN

Comparison of graphical optimization or IPSA for improving brachytherapy plans associated with inadequate target coverage for cervical cancer

ZhiJie Liu¹, HuanQing Liang², Xiao Wang³, HaiMing Yang¹, Ye Deng¹, TingJun Luo¹, ChaoFeng Yang¹, Min Lu¹, QingGuo Fu¹ & XiaoDong Zhu¹

Many studies have reported that inverse planning by simulated annealing (IPSA) can improve the quality of brachytherapy plans, and we wanted to examine whether IPSA could improve cervical cancer brachytherapy plans giving $D_{90} < 6$ Gy (with 7 Gy per fraction) at our institution. Various IPSA plans involving the tandem and ovoid applicators were developed for 30 consecutive cervical cancer patients on the basis of computed tomography: IPSA1, with a constraint on the maximum dose in the target volume; IPSA1-0, identical to IPSA1 but without a dwell-time deviation constraint; IPSA2, without a constraint on the maximum dose; and IPSA2-0, identical to IPSA2 but without a dwell-time deviation constraint. IPSA2 achieved similar results as graphical optimization, and none of the other IPSA plans was significantly better than graphical optimization. Therefore, other approaches, such as combining interstitial and intracavitary brachytherapy, may be more appropriate for improving the quality of brachytherapy plans associated with inadequate target coverage.

Cervical cancer is very common in China, and brachytherapy plays an important role in its treatment¹. Brachytherapy plans were historically developed using radiographs and point dosimetry systems², and today 3-D image-guided brachytherapy is used to optimize the dose distribution to the target volume and avoid high doses to organs at risk^{3–5}. Inverse planning by simulated annealing (IPSA) can allow the use of lower radiation doses while maintaining or improving target coverage when planning brachytherapy involving tandem and ovoid applicators in cervical cancer⁶. Other studies have reported similar results when comparing IPSA with dose point optimization, manual optimization of dwell weights/times and geometric optimization for planning brachytherapy involving a tandem and ovoid^{7–11}.

In our hospital, some brachytherapy plans based on the graphical optimization (GrO) algorithm do not give adequate target coverage (providing $D_{90} < 6$ Gy and 7 Gy per fraction) when the dose to organs at risk is kept within recommended limits routinely used at our institution. Here we investigated whether such plans could be improved using IPSA. Our primary criterion for improvement was D_{90} , and secondary criteria were V_{150} , V_{200} and dwell time.

Results

Comparison of IPSA1, IPSA2 and GrO. Mean D_{90} was 0.2 Gy smaller with IPSA1 than with GrO (3.8%, $p = 0.031$; Table 1 and Fig. 1), while D_{90} was 0.4 Gy higher with IPSA2 than with IPSA1 (8.0%, $p = 0.002$),

¹Department of Radiation Oncology, Cancer Institute of Guangxi Zhuang Autonomous Region, The Affiliated Cancer Hospital of Guangxi Medical University, Nanning, 530021, PR China. ²Department of Radiation Oncology, Nanfang Hospital, Southern Medical University, Guangzhou, 510515, PR China. ³Department of Radiation Oncology, Rutgers Cancer Institute of New Jersey, New Brunswick, NJ, 08903, USA. ZhiJie Liu and HuanQing Liang contributed equally to this work. Correspondence and requests for materials should be addressed to Q.F. (email: fqg801219@126.com) or X.Z. (email: zhuxdongxmu@126.com)

parameters	GrO	IPSA1	IPSA2	IPSA1-0	IPSA2-0	p value
D100(Gy)	3.2 ± 0.5	3.1 ± 0.6	3.5 ± 0.5 ^{a,c,d}	3.4 ± 0.5 ^{a,c,d}	3.6 ± 0.5 ^{a,b,c}	0.042
D90(Gy)	5.2 ± 0.6	5.0 ± 0.6 ^e	5.4 ± 0.6 ^a	5.2 ± 0.6 ^{b,d}	5.4 ± 0.6 ^a	0.038
V100(%)	66.2 ± 8.8	62.7 ± 9.7 ^e	68.0 ± 9.4 ^a	65.9 ± 8.8 ^{b,d}	68.8 ± 9.2 ^a	0.036
V150(%)	35.9 ± 5.8	33.4 ± 6.7 ^e	35.8 ± 5.6	34.7 ± 5.5 ^e	36.2 ± 5.6	0.022
V200(%)	21.9 ± 3.5	19.6 ± 3.7 ^e	21.4 ± 3.4	20.7 ± 3.5 ^e	21.7 ± 3.4	0.041
CNI	0.62 ± 0.08 ^e	0.57 ± 0.09 ^e	0.59 ± 0.09	0.58 ± 0.08	0.60 ± 0.09	0.042
CI	0.94 ± 0.06 ^e	0.91 ± 0.04 ^e	0.87 ± 0.06	0.89 ± 0.04 ^e	0.87 ± 0.06	0.016
Bladder2cc(Gy)	4.4 ± 0.1 ^e	4.5 ± 0.03	4.5 ± 0.07	4.5 ± 0.04	4.5 ± 0.08	0.027
Rectum2cc(Gy)	3.6 ± 0.4	3.4 ± 0.4 ^e	3.5 ± 0.4	3.5 ± 0.4	3.6 ± 0.4	0.044
Sigmoid2cc(Gy)	2.7 ± 1.0	2.5 ± 0.9	2.7 ± 1.0	2.7 ± 1.0	2.8 ± 1.0	0.653
Total dwell time(s)	587.1 ± 304.9 ^e	565.1 ± 289.4 ^e	632.0 ± 324.8	602.7 ± 305.5 ^e	643.0 ± 330.3	0.002
Max dwell time(s)	54.2 ± 66.9	50.8 ± 35.5	68.0 ± 35.5	111.8 ± 75.4 ^e	74.2 ± 53.1	0.000
SD of dwell time (s)	12.6 ± 13.7	13.3 ± 9.2	18.0 ± 15.3 ^{a,c}	22.8 ± 14.7 ^e	19.0 ± 13.2 ^{a,c}	0.003

Table 1. Comparison of results with each plan. Results are mean ± 1 standard deviation. ^aSignificantly different from the GrO. ^bSignificantly different from the IPSA2. ^cSignificantly different from the IPSA1. ^dSignificantly different from the IPSA2-0. ^eSignificantly different from all other plans.

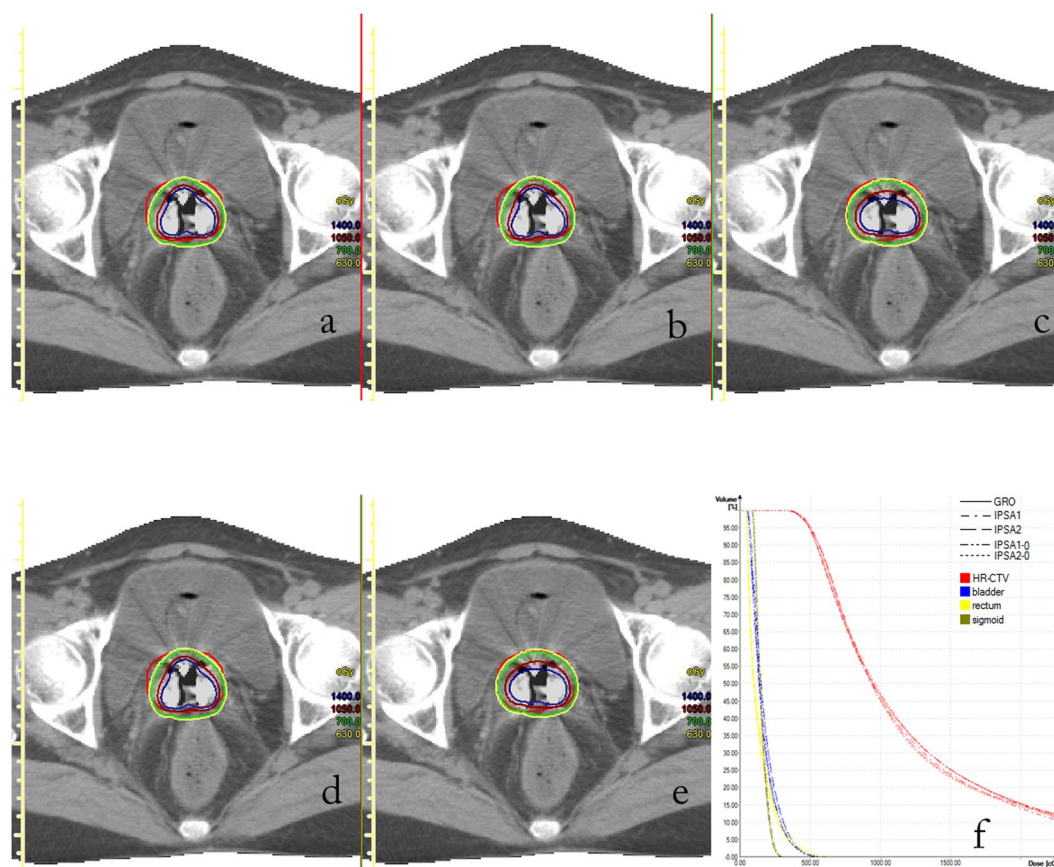


Figure 1. Example of transverse computed tomography images and dose-volume histogram from one patient for brachytherapy planned using (a) GrO, (b) IPSA1, (c) IPSA2, (d) IPSA1-0, or (e) IPSA2-0. (f) The dose-volume histogram.

illustrating the effect of removing the V_{\max} restriction. Of the three planning algorithms, IPSA1 had the smallest V_{150} and V_{200} ($p = 0.036$ and 0.030 vs. GrO; $p = 0.037$ and 0.032 vs. IPSA2).

A direct linear relationship was observed between high-risk clinical target volume (HR-CTV) D_{90} and high dose in the target (Fig. 2). The IPSA2 line lies beneath the two straight lines of IPSA1 and GrO indicating that IPSA2 may be associated with smaller V_{150} than IPSA1 or GrO for the same HR-CTV D_{90} . The length of each line represents the range of the HR-CTV D_{90} , and a considerable part of the line in the case of IPSA1 is biased towards the left side of the x axis, indicating that it provided the smallest average high-dose volume. Lines for the various IPSA algorithms nearly coincide for V_{200} .

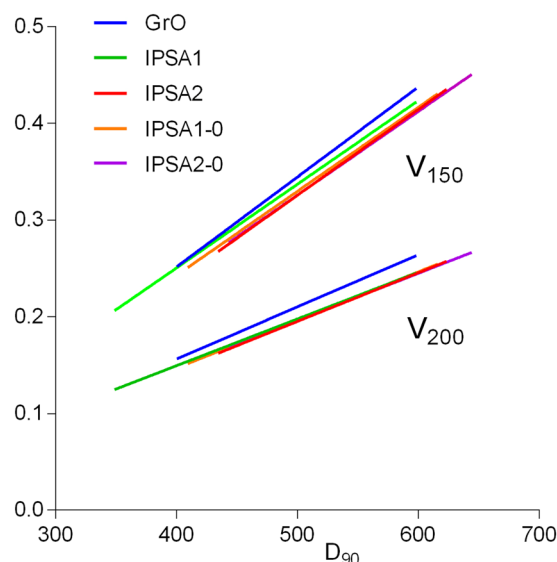


Figure 2. Linear relationship among D_{90} , V_{150} and V_{200} .

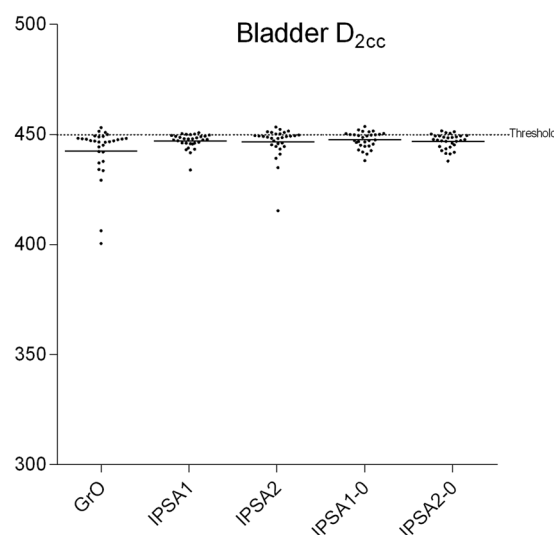


Figure 3. Comparison of bladder D_{2cc} among different plans.

Figures 3–5 show that the concentration of D_{2cc} points near the dose limit is greater at the bladder than at other organs at risk. This indicates that all the plans tested expose the bladder to a similar dose, implying that the bladder may be the organ at risk that most limits target coverage. GrO offered significantly lower dose to the bladder than the IPSA plans ($p = 0.012$), whereas IPSA1 offered significantly lower dose to the rectum ($p = 0.001$).

The conformity index (CI) of GrO was 0.94; IPSA1, 0.91; and IPSA2, 0.87 ($p = 0.002$; Table 1). The corresponding values of the conformal index (COIN) were 0.62, 0.57 and 0.59 ($p = 0.000$). There was no significant difference in maximum dwell time among the three plans ($p = 0.526$), although IPSA2 showed significantly longer total dwell time and greater dwell-time standard deviation than the two other methods ($p = 0.002$, $p = 0.003$).

Comparing IPSA plans with and without dwell-time deviation constraint. There was significant difference in D_{90} between IPSA1 and IPSA1-0 ($p = 0.047$) while there was no significant difference between IPSA2 and IPSA2-0 ($p = 0.781$). The V_{150} and V_{200} of IPSA1-0 were significantly higher than those of IPSA1 (34.7% vs 33.4%, $p = 0.001$; 20.7% vs 19.6%, $p = 0.013$). COIN and CI were also significantly different between IPSA1-0 and IPSA1 ($p = 0.026$, $p = 0.001$).

Total dwell time, maximum dwell time and dwell-time standard deviation were significantly larger with IPSA1-0 than with IPSA1 ($p = 0.003$, $p = 0.000$, $p = 0.000$), reflecting the lack of a constraint on dwell-time deviation. These three parameters did not differ significantly between IPSA2-0 and IPSA2 ($p = 0.642$, $p = 0.574$, $p = 0.663$).

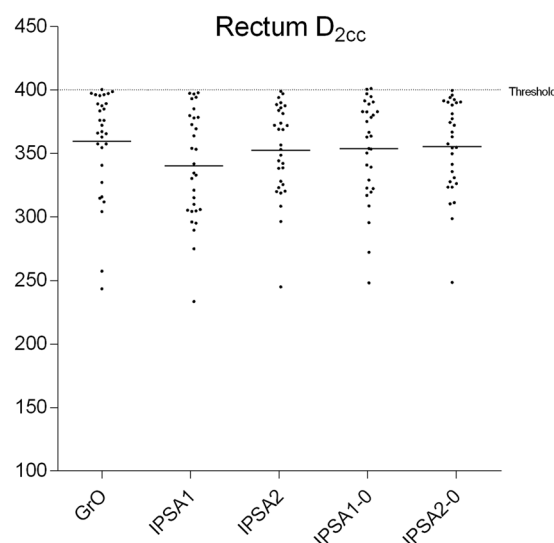


Figure 4. Comparison of rectum D_{2cc} among different plans.

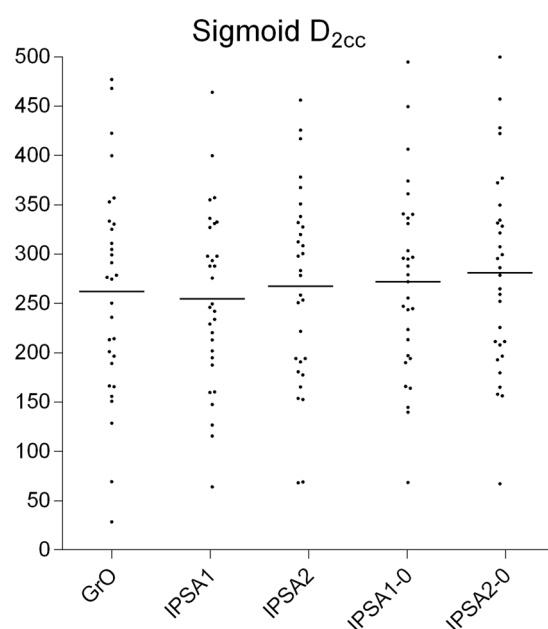


Figure 5. Comparison of sigmoid D_{2cc} among different plans.

Discussion

The IPSA1 plan did not provide better target coverage than GrO. The IPSA2 plan improved D_{90} by 0.4 Gy (8%) relative to IPSA1, reflecting the effect of removing the V_{max} restriction; however, this improved D_{90} by only 0.2 Gy relative to GrO. Further removing the dwell-time deviation constraint led to increases in V_{150} , V_{200} , total dwell time, maximum dwell time and dwell-time standard deviation.

We found a linear relationship between D_{90} and high dose at the target (Fig. 2). This likely reflects a fundamental limitation of the tandem and ovoid applicators: since only one catheter lies within the uterine cavity, the isodose lines form concentric circles around it, reflecting the fact that dose falls off by the inverse square law. As a result, achieving the prescribed dose on the surface of a large target necessarily implies a large high-dose volume at the target.

The optimization parameter V_{max} in IPSA1 may not be the most effective guide for brachytherapy planning, since it operates in opposition to the “minimum surface dose” parameter. Dose distribution is quite sensitive to V_{max} , which can decrease dose to organs at risk, high-dose volume in the target as well as target coverage¹². We found that removing the V_{max} constraint improved target coverage while keeping the dose to organs at risk within limits. Thus, IPSA2 showed greater V_{150} and V_{200} than IPSA1 while keeping the high-dose volume similar to that with GrO. These results suggest that the “maximum surface dose” parameter used in IPSA2 may be more reasonable and effective.

	Plan	Region of interest	Surface dose				Volume dose			
			Weight	Min dose	Max dose	Weight	Weight	Min dose	Max dose	Weight
Target	IPSA1	HR-CTV	170	7.0 Gy	7.5 Gy	100	100	7.2 Gy	80.0 Gy	5
	IPSA2	HR-CTV	150	7.0 Gy	7.5 Gy	100	100	7.2 Gy		
Organs at risk		Bladder			4.0 Gy	100				
		Rectum			3.5 Gy	50				
		Sigmoid			4.0 Gy	30				

Table 2. Dose objectives and weighting factors used for IPSA plans.

At the same time, removing the V_{\max} restraint increased target coverage by 0.2 Gy relative to GrO, which does not substantially improve plan quality. In fact, the various IPSA plans succeeded only in optimizing dwell time and dwell position relative to GrO. In all plans, a large part of the target lies close to the bladder or rectum, or the target extends laterally into the region in the case of a tandem applicator. This suggests that dose distribution is affected mainly by the location of the target and organs at risk, the shape of the target and the placement of the catheters. If all these factors are fixed, optimization of dwell time and dwell position can, at best, merely fine-tune the dose distribution. These findings are consistent with other studies showing that IPSA can minimize dose to organs at risk and maximize target coverage without substantially altering the dose distribution in brachytherapy for prostate cancer^{13,14} or gynecologic cancers^{7,8,10}.

Using different applicators may substantially improve plan quality. In contrast to our increase of 0.2 Gy in mean D_{90} achieved through plan optimization, the combination of interstitial and intracavitary brachytherapy can increase D_{90} by about 1 Gy (17.5%) relative to intracavitary brachytherapy alone¹¹. Similarly, using Vienna applicators rather than tandem and ovoid applicators increased D_{90} by 1.7 Gy (27.9%)⁹, and interstitial brachytherapy has been shown to give higher mean D_{90} than intracavitary brachytherapy¹⁵.

We found that removing the dwell-time deviation constraint from IPSA1 and IPSA2 increased target coverage and dwell-time deviation, consistent with a previous report¹⁶. However, the change in D_{90} was relatively small in our study. In addition, the increase in dwell-time deviation can generate isolated dwell positions with long dwell times, which may increase the risk of hot spots. These hot spots may migrate onto organs at risk if the catheter shifts after computed tomography. Therefore, removing the dwell-time deviation constraint may not be an appropriate method for improving target coverage.

IPSA2 significantly increased target coverage without increasing V_{150} or V_{200} relative to GrO. At the same time, IPSA2 showed larger dwell-time deviation than GrO and IPSA1. Increasing the dwell-time deviation constraint may reduce dwell-time deviation in IPSA2¹⁶.

Although our results reflect the particular approach for target delineation and plan evaluation in place at our hospital, our findings may be useful for brachytherapy planning at other institutions. We found that none of the IPSA plans substantially improved brachytherapy quality above GrO, and the IPSA2 plan achieved similar results as GrO. The “maximum surface dose” parameter may be more reasonable and effective for decreasing high dose volume of brachytherapy plans giving poor performance ($D_{90} < 6$ Gy with 7 Gy per fraction) using tandem and ovoid applicators. Removing the dwell-time deviation constraint may increase the risk of harm to normal tissue without improving target coverage.

Methods

Patients. Computed tomography images were used to re-plan the brachytherapy treatment plans based on tandem and ovoid applicators for 30 consecutive patients (mean age, 48 yr) with cervical cancer in stage IIB–IIIB based on the International Federation of Gynecology and Obstetrics staging system. These patients were treated at the Affiliated Cancer Hospital of Guangxi Medical University between December 2015 and June 2016. Patients were treated with external beam radiation therapy of 50 Gy in 25 fractions to the target and were concurrently given chemotherapy. This combination therapy was followed by high-dose-rate brachytherapy of 28 Gy in 4–5 fractions.

This study was approved by the Ethics Committee at the Affiliated Cancer Hospital of Guangxi Medical University. All procedures were in accordance with national and international ethical guidelines. Informed consent was obtained from all participants.

Contouring. Each brachytherapy fraction was followed by computed tomography scanning and contour delineation. Therefore, every patient had four or five computed tomography image sets and contours of the region of interest. Only one fraction from each patient was used in this study. HR-CTVs and organs at risk (rectum, bladder and sigmoid)¹⁷ were delineated by a gynecologist.

Contouring and treatment planning were performed using Oncentra® Brachy software (version 4.3, Elekta). One GrO plan and four IPSA plans (see below) were prepared from each computed tomography image set. HR-CTV per fraction was defined to be 7 Gy, maximum bladder dose could not exceed 4.5 Gy, and maximum rectum dose could not exceed 4 Gy. In some cases, limiting the dose to organs at risk was given higher priority than target coverage. This was decided by the physician based on prognostic factors and institutional procedures. When target coverage was insufficient, an additional fraction of high-dose-rate brachytherapy was delivered in order to cover the target with an equivalent dose in 2 Gy-fractions (EQD2) of 80–90 Gy.

Treatment planning. *GrO plans.* GrO plans were first optimized via dose points optimization. After digitizing applicators, the dwell positions, separated by a 2.5-mm step size, were determined by the extent of the

HR-CTV. Dose distributions were then dose-points-optimized with 300 target points randomly placed at the surface of the HR-CTV. After dose points optimization, the GrO was applied to adjust isodose lines using the mouse to achieve the desired target coverage while keeping the doses to organs at risk below the given constraints. The GrO plans were used in actual treatments.

IPSA plans. Two-class solutions shown in Table 2 were used as starting points for IPSA1 and IPSA2. The main differences between IPSA1 and IPSA2 were that IPSA1 had a constraint on the maximum dose to the target volume (V_{\max}), and IPSA1 assigned a slightly higher weight to the “minimum surface dose” parameter. The dwell-time deviation constraint was set to 0.2 in both IPSA1 and IPSA2. To further improve target coverage, this constraint was set to 0 in these plans to generate the respective plans IPSA1-0 and IPSA2-0. The organs at risk were set to the same value in the two-class solutions. After running the optimization with the class solution, dose objectives and weighting factors were modified for individual patients when necessary in order to optimize the dose distribution. After the final results were obtained in the IPSA plans, no fine-tuning of the dose distribution using GrO was allowed.

Plan evaluation. The following dosimetric parameters of different plans were analyzed based on the dose-volume histograms: HR-CTV D_{90} , the dose that covered 90% of the HR-CTV; D_{100} , the dose that covered 100% of the HR-CTV; V_{100} , the percentage volume covered by at least 100% of the prescribed dose; V_{150} , the volume that received at least 150% of the prescribed dose; V_{200} , the volume that received at least 200% of the prescribed dose; and D_{2cc} , dose covering at least 2 cm³ of organs at risk. In addition, COIN and CI⁷, were compared (Eqs 1–2).

Since we were concerned about potential hot spots, we also evaluated the differences in dwell time distributions by recording the mean and maximum dwell time and the mean standard deviation (SD) of the dwell time in each plan.

Statistical analysis. Differences in the means of each dose parameter among the five plans (GrO, IPSA1, IPSA2, IPSA1-0, IPSA2-0) were assessed for significance using matched ANOVA. Two-group comparisons were assessed for significance using the least-squares difference test. Two-tailed values of $P < 0.05$ were considered statistically significant. All data analyses were performed using SPSS (IBM, Chicago, IL, USA) and GraphPad Prism 5 (Graphpad, USA).

Data availability. The datasets analyzed in the present study are available from the corresponding author upon reasonable request.

$$\text{COIN} = \text{CTV}_{\text{target}} \times \text{CTV}_{\text{target}} / (V_{\text{CTV}} \times V_{\text{total}}) \quad (1)$$

$$\text{CI} = \text{CTV}_{\text{target}} / V_{\text{total}} \quad (2)$$

$\text{CTV}_{\text{target}}$ is the part of the HR-CTV receiving at least the prescribed dose, V_{total} is the total volume receiving at least the prescribed dose, and V_{CTV} is the volume of the HR-CTV.

References

- Viswanathan, A. N. *et al.* American Brachytherapy Society consensus guidelines for locally advanced carcinoma of the cervix. Part II: high-dose-rate brachytherapy. *Brachytherapy* **11**, 47–52, <https://doi.org/10.1016/j.brachy.2011.07.002> (2012).
- Brooks, S., Bownes, P., Lowe, G., Bryant, L. & Hoskin, P. J. Cervical brachytherapy utilizing ring applicator: comparison of standard and conformal loading. *International journal of radiation oncology, biology, physics* **63**, 934–939, <https://doi.org/10.1016/j.ijrobp.2005.07.963> (2005).
- De Brabandere, M., Mousa, A. G., Nulens, A., Swinnen, A. & Van Limbergen, E. Potential of dose optimisation in MRI-based PDR brachytherapy of cervix carcinoma. *Radiotherapy and oncology: journal of the European Society for Therapeutic Radiology and Oncology* **88**, 217–226, <https://doi.org/10.1016/j.radonc.2007.10.026> (2008).
- Lindgaard, J. C., Tanderup, K., Nielsen, S. K., Haack, S. & Gelineck, J. MRI-guided 3D optimization significantly improves DVH parameters of pulsed-dose-rate brachytherapy in locally advanced cervical cancer. *International journal of radiation oncology, biology, physics* **71**, 756–764, <https://doi.org/10.1016/j.ijrobp.2007.10.032> (2008).
- Potter, R. *et al.* Clinical impact of MRI assisted dose volume adaptation and dose escalation in brachytherapy of locally advanced cervix cancer. *Radiotherapy and oncology: journal of the European Society for Therapeutic Radiology and Oncology* **83**, 148–155, <https://doi.org/10.1016/j.radonc.2007.04.012> (2007).
- Dewitt, K. D. *et al.* 3D inverse treatment planning for the tandem and ovoid applicator in cervical cancer. *International journal of radiation oncology, biology, physics* **63**, 1270–1274, <https://doi.org/10.1016/j.ijrobp.2005.07.972> (2005).
- Palmqvist, T. *et al.* Dosimetric evaluation of manually and inversely optimized treatment planning for high dose rate brachytherapy of cervical cancer. *Acta oncologica (Stockholm, Sweden)* **53**, 1012–1018, <https://doi.org/10.3109/0284186x.2014.928829> (2014).
- Chajon, E. *et al.* Inverse planning approach for 3-D MRI-based pulse-dose rate intracavitary brachytherapy in cervix cancer. *International journal of radiation oncology, biology, physics* **69**, 955–961, <https://doi.org/10.1016/j.ijrobp.2007.07.2321> (2007).
- Jamema, S., Mahantshetty, U., Deshpande, D., Sharma, S. & Shrivastava, S. Does help structures play a role in reducing the variation of dwell time in IPSA planning for gynaecological brachytherapy application? *Journal of contemporary brachytherapy* **3**, 142–149, <https://doi.org/10.5114/jcb.2011.24821> (2011).
- Jamema, S. V. *et al.* Comparison of IPSA with dose-point optimization and manual optimization for interstitial template brachytherapy for gynecologic cancers. *Brachytherapy* **10**, 306–312, <https://doi.org/10.1016/j.brachy.2010.08.011> (2011).
- Yoshio, K. *et al.* Inverse planning for combination of intracavitary and interstitial brachytherapy for locally advanced cervical cancer. *Journal of radiation research* **54**, 1146–1152, <https://doi.org/10.1093/jrr/rrr072> (2013).
- Lapuz, C., Dempsey, C., Capp, A. & O'Brien, P. C. Dosimetric comparison of optimization methods for multichannel intracavitary brachytherapy for superficial vaginal tumors. *Brachytherapy* **12**, 637–644, <https://doi.org/10.1016/j.brachy.2013.04.009> (2013).

13. Morton, G. C., Sankrecha, R., Halina, P. & Loblaw, A. A comparison of anatomy-based inverse planning with simulated annealing and graphical optimization for high-dose-rate prostate brachytherapy. *Brachytherapy* 7, 12–16, <https://doi.org/10.1016/j.brachy.2007.10.001> (2008).
14. Panettieri, V., Smith, R. L., Mason, N. J. & Millar, J. L. Comparison of IPSA and HIPO inverse planning optimization algorithms for prostate HDR brachytherapy. *Journal of applied clinical medical physics/American College of Medical Physics* 15, 5055, <https://doi.org/10.1120/jacmp.v15i6.5055> (2014).
15. Liu, Z. S. *et al.* Computed Tomography-Guided Interstitial Brachytherapy for Locally Advanced Cervical Cancer: Introduction of the Technique and a Comparison of Dosimetry With Conventional Intracavitary Brachytherapy. *International journal of gynecological cancer: official journal of the International Gynecological Cancer Society* 27, 768–775, <https://doi.org/10.1097/igc.0000000000000929> (2017).
16. Smith, R. L. *et al.* The influence of the dwell time deviation constraint (DTDC) parameter on dosimetry with IPSA optimisation for HDR prostate brachytherapy. *Australasian physical & engineering sciences in medicine/supported by the Australasian College of Physical Scientists in Medicine and the Australasian Association of Physical Sciences in Medicine* 38, 55–61, <https://doi.org/10.1007/s13246-014-0317-2> (2015).
17. Potter, R. *et al.* Recommendations from gynaecological (GYN) GEC ESTRO working group (II): concepts and terms in 3D image-based treatment planning in cervix cancer brachytherapy-3D dose volume parameters and aspects of 3D image-based anatomy, radiation physics, radiobiology. *Radiotherapy and oncology: journal of the European Society for Therapeutic Radiology and Oncology* 78, 67–77, <https://doi.org/10.1016/j.radonc.2005.11.014> (2006).

Acknowledgements

This work was supported in part by the Self-financing Project of Guangxi Zhuang Autonomous Region Health and Family Planning Commission (Z2016481) and the Guangxi Medical University Youth Science Foundation (GXMUYSF201627).

Author Contributions

Liu Zhijie prepared the brachytherapy plans, participated in data collection and data analysis, and co-wrote the manuscript. Liang Huanqing participated in data collection and data analysis, and co-wrote the manuscript. Wang Xiao co-wrote the manuscript. Yang Haiming, Deng Ye, Luo Tingjun, Yang Chaofeng and Lu Min participated in data collection. Fu Qingguo and Zhu XiaoDong designed the study.

Additional Information

Competing Interests: The authors declare that they have no competing interests.

Publisher's note: Springer Nature remains neutral with regard to jurisdictional claims in published maps and institutional affiliations.



Open Access This article is licensed under a Creative Commons Attribution 4.0 International License, which permits use, sharing, adaptation, distribution and reproduction in any medium or format, as long as you give appropriate credit to the original author(s) and the source, provide a link to the Creative Commons license, and indicate if changes were made. The images or other third party material in this article are included in the article's Creative Commons license, unless indicated otherwise in a credit line to the material. If material is not included in the article's Creative Commons license and your intended use is not permitted by statutory regulation or exceeds the permitted use, you will need to obtain permission directly from the copyright holder. To view a copy of this license, visit <http://creativecommons.org/licenses/by/4.0/>.

© The Author(s) 2017